ESI for

Photostable ester-substituted bis-cyclometalated cationic iridium(III) complexes

for continuous monitoring oxygen

Chun Liu*, Hongcui Yu, Yang Xing, Zhanming Gao and Zilin Jin

[*] Dr. C. Liu, Corresponding Author
State Key Laboratory of Fine Chemicals, Dalian University of Technology, Linggong
Road 2, Dalian 116024, China.
Tel.: +86-411-84986182.
E-mail: cliu@dlut.edu.cn

Content

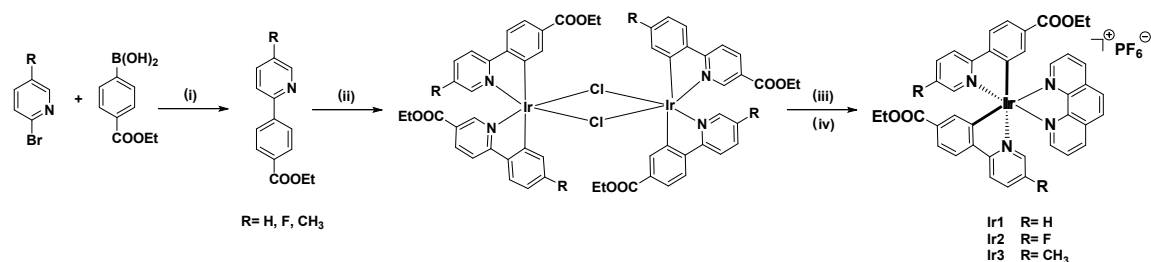# Synthetic method and characterization of ligands and iridium(III) complexes

**Scheme S1** Synthetic routes of the cyclometalated iridium(III) complexes for this study. (i) Pd(PPh₃)₄, Na₂CO₃, THF/H₂O 3 : 1 (v/v), 80 °C, N₂, 12h; (ii) IrCl₃·3H₂O, EtOCH₂CH₂OH/H₂O 3 : 1 (v/v), 120 °C, N₂, 24 h; (iii) 1,10-Phenanthroline, CH₂Cl₂/MeOH, 2 : 1 (v/v), 50°C, N₂, 12h; (iv) KPF₆, RT, 1 h.

Ligands and iridium(III) complexes were synthesized according to the literature methods for analogous compounds.[1] The whole synthesis route for iridium(III) complexes was shown in Scheme S1. For the sake of clarity and simplicity, the following abbreviations for the different C^N ligand containing ester group are used throughout: **epbz1** for ethyl 4-(2-pyridinyl) benzoate, **epbz2** for ethyl 4-(5-fluoro-2-pyridinyl) benzoate, **epbz3** for ethyl 4-(5-methyl-2-pyridinyl) benzoate; **Ir1** for [Ir(**epbz1**)₂(phen)]⁺PF₆⁻, **Ir2** for [Ir(**epbz2**)₂(phen)]⁺PF₆⁻, and **Ir3** for [Ir(**epbz3**)₂(phen)]⁺PF₆⁻.
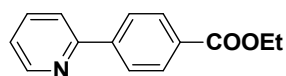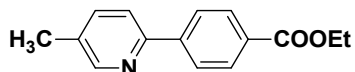

epbz1: yield: 87.7%; a white solid.
^{1}H NMR (400 MHz, DMSO-d_6): δ = 8.72 (d, J = 4.6 Hz, 1H), 8.24 (d, J = 8.5 Hz, 2H), 8.07 (d, J = 4.2 Hz, 3H), 7.93 (t, J = 8.6 Hz, 1H), 7.47 – 7.36 (m, 1H), 4.34 (q, J = 7.1 Hz, 2H), 1.34 (t, J = 7.1 Hz, 3H).
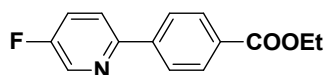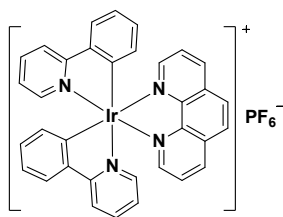

epbz2: yield: 86.9%; a white solid.
^{1}H NMR (400 MHz, DMSO-d_6): δ = 8.71 (d, J = 2.9 Hz, 1H), 8.19 (t, J = 8.7 Hz, 2H), 8.15 (dd, J = 8.9 Hz, 4.3 Hz, 1H), 8.06 (dd, J = 8.5 Hz, 2.0 Hz, 2H), 7.88 (td, J = 8.6 Hz, 2.7 Hz, 1H), 4.34 (q, J = 7.1 Hz, 2H), 1.34 (t, J = 7.1 Hz, 3H).
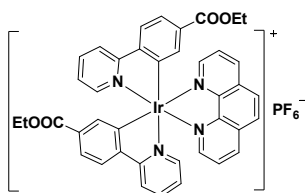

epbz3: yield: 78.3%; a white solid.
^{1}H NMR (400 MHz, DMSO-d_6): δ = 8.56 (s, 1H), 8.21 (d, J = 8.5 Hz, 2H), 8.05 (d, J = 8.4 Hz, 2H), 7.96 (d, J = 8.1 Hz, 1H), 7.75 (dd, J = 8.1 Hz, 1.6 Hz, 1H), 4.34 (q, J = 7.1 Hz, 2H), 2.36 (s, 3H), 1.35 (t, J = 7.1 Hz, 3H).

Ir0: Yield: 70.4%; a yellow solid.

^{1}H NMR (400 MHz, DMSO-d_6): δ = 8.90 (d, J = 8.2 Hz, 2H), 8.39 (s, 2H), 8.23 (dd, J = 22.8 Hz, 6.5 Hz, 4H), 8.05 (dd, J = 8.2 Hz, 5.1 Hz, 2H), 7.95 (d, J = 7.7 Hz, 2H), 7.87 (t, J = 7.8 Hz, 2H), 7.46 (d, J = 5.7 Hz, 2H), 7.06 (t, J = 7.5 Hz, 2H), 7.02 − 6.91 (m, 4H), 6.29 (d, J = 7.5 Hz, 2H).

Ir1: Yield: 68.2%; a yellow solid.

^{1}H NMR (400 MHz, DMSO-d_6): δ = 8.92 (d, J = 8.4 Hz, 2H), 8.41 (d, J = 7.0 Hz, 4H), 8.24 − 8.19 (m, 2H), 8.10 (d, J = 8.3 Hz, 2H), 8.06 − 7.95 (m, 4H), 7.67 − 7.52 (m, 4H), 7.13 (t, J = 6.6 Hz, 2H), 6.87 (d, J = 1.6 Hz, 2H), 4.14 (q, J = 7.0 Hz, 4H), 1.17 (t, J = 7.1 Hz, 6H).

^{13}C NMR (100 MHz, DMSO-d_6): δ = 166.5, 166.4, 150.8, 149.5, 149.2, 148.2, 148.2, 146.7, 139.3, 138.5, 132.3, 131.8, 131.6, 128.9, 126.6, 124.7, 124.4, 120.8, 60.9, 14.2.

HRMS (m/z; EI): calcd. for $C_{40}H_{32}N_4O_4Ir$ [M − PF$_6$]$^+$ 825.2053; found 825.2122.
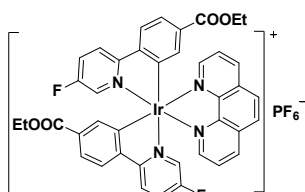
Ir2: Yield: 58.4%; a yellow-green solid.

^{1}H NMR (400 MHz, DMSO-d_6): δ = 8.91 (dd, J = 8.3 Hz, 1.3 Hz, 2H), 8.52 (dd, J = 9.2 Hz, 5.4 Hz, 2H), 8.39 (s, 2H), 8.17 (dd, J = 5.1 Hz, 1.2 Hz, 2H), 8.11 (dd, J = 11.3 Hz, 5.5 Hz, 4H), 8.01 (dd, J = 8.3 Hz, 5.1 Hz, 2H), 7.68 − 7.58 (m, 4H), 6.85 (d, J = 1.6 Hz, 2H), 4.16 (q, J = 7.1 Hz, 4H), 1.19 (t, J = 7.1 Hz, 6H).

^{13}C NMR (100 MHz, DMSO-d_6) δ = 165.4, 162.8, 159.3, 157.3, 151.2, 147.8, 146.3, 139.1, 138.6, 138.3, 131.4, 130.3, 128.3, 127.2, 127.0, 125.1, 123.7, 122.7, 60.4, 14.2.

HRMS (m/z; EI): calcd. for $C_{40}H_{30}F_2N_4O_4Ir$ [M − PF$_6$]$^+$ 861.1864; found 861.1914.
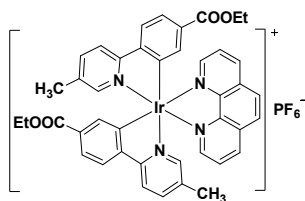
Ir3: Yield 61.3%; a yellow solid.

^{1}H NMR (400 MHz, DMSO-d_6): δ = 8.91 (dd, J = 8.3 Hz, 1.2 Hz, 2H), 8.40 (s, 2H), 8.31 (d, J = 8.5 Hz, 2H), 8.20 (dd, J = 5.1 Hz, 1.3 Hz, 2H), 8.04 (dd, J = 8.3 Hz, 4.4 Hz, 4H), 7.86 (d, J = 9.5 Hz, 2H), 7.61 (dd, J = 8.1 Hz, 1.6 Hz, 2H), 7.30 (s, 2H), 6.85 (d, J = 1.6 Hz, 2H), 4.13 (q, J = 7.1 Hz, 4H), 2.01 (s, 6H), 1.18 (t, J = 7.1 Hz, 6H).

^{13}C NMR (100 MHz, DMSO-d_6): δ = 166.0, 163.5, 151.4, 149.6, 149.3, 148.8, 146.6, 140.3, 139.4, 135.6, 131.9, 131.6, 130.4, 128.8, 127.7, 125.0, 124.0, 121.4, 60.9, 18.0, 14.4.

HRMS (m/z; EI): calcd. for $C_{42}H_{36}N_4O_4Ir$ [M – PF$_6$]$^+$ 853.2366; found 853.2413.

Table S1. Crystallographic data for **Ir2**.

Empirical formula	$C_{48}H_{50}F_8IrN_4O_5P$
Formula weight	1138.09
Crystaltemperature (K)	296(2)
Crystal system	Monoclinic
Space group	P2/n
Z	2
a(Å)	15.1089(4)
b(Å)	11.0424(3)
c(Å)	15.6517(4)
α(deg)	90.00
β(deg)	110.4110(10)
γ(deg)	90.00
V(Å^3)	2447.35(11)
D$_x$(Mg.cm^{-3})	1.544
μ(mm^{-1})	1.285
F(000)	1140.0
R$_{int}$	0.0225
No.of collected data(unique)	4292
No.of parameters varied	371
s	1.039
final R indices [I >2σ(I)]	0.0334
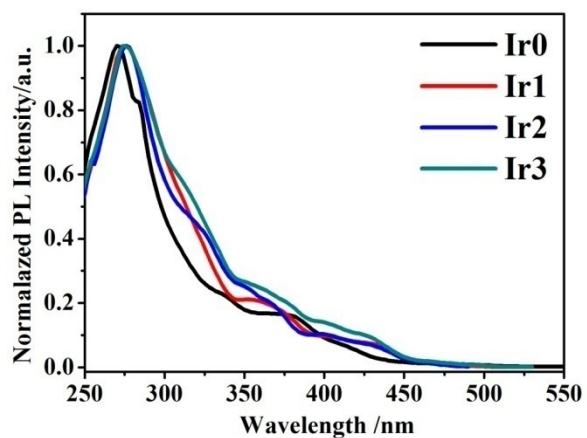
Fig. S1. Photoluminescence excitation spectra of **Ir0~Ir3** in CH$_2$Cl$_2$.
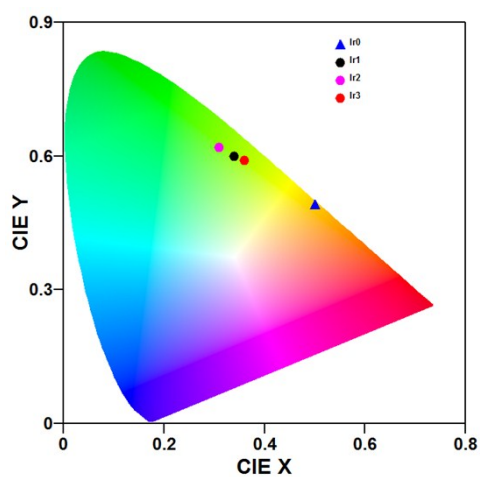

Fig. S2. CIE Plots for **Ir0** (0.50, 0.49), **Ir1** (0.34, 0.60), **Ir2** (0.31, 0.62), and **Ir3** (0.36, 0.59).
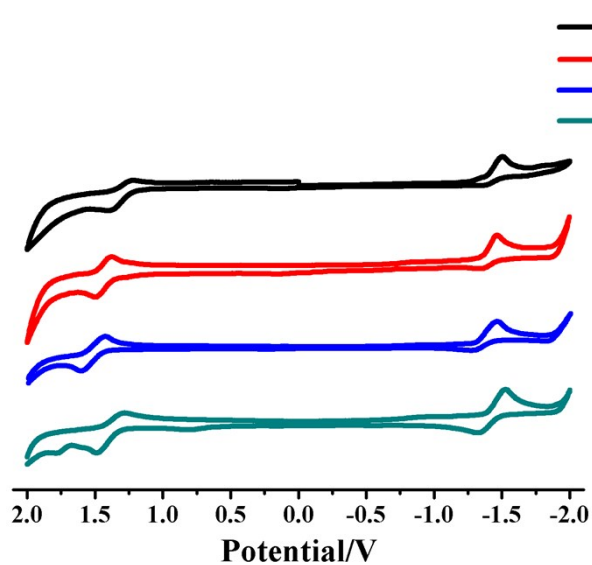

Fig. S3. Cyclic voltamograms for complexes **Ir0~Ir3**.
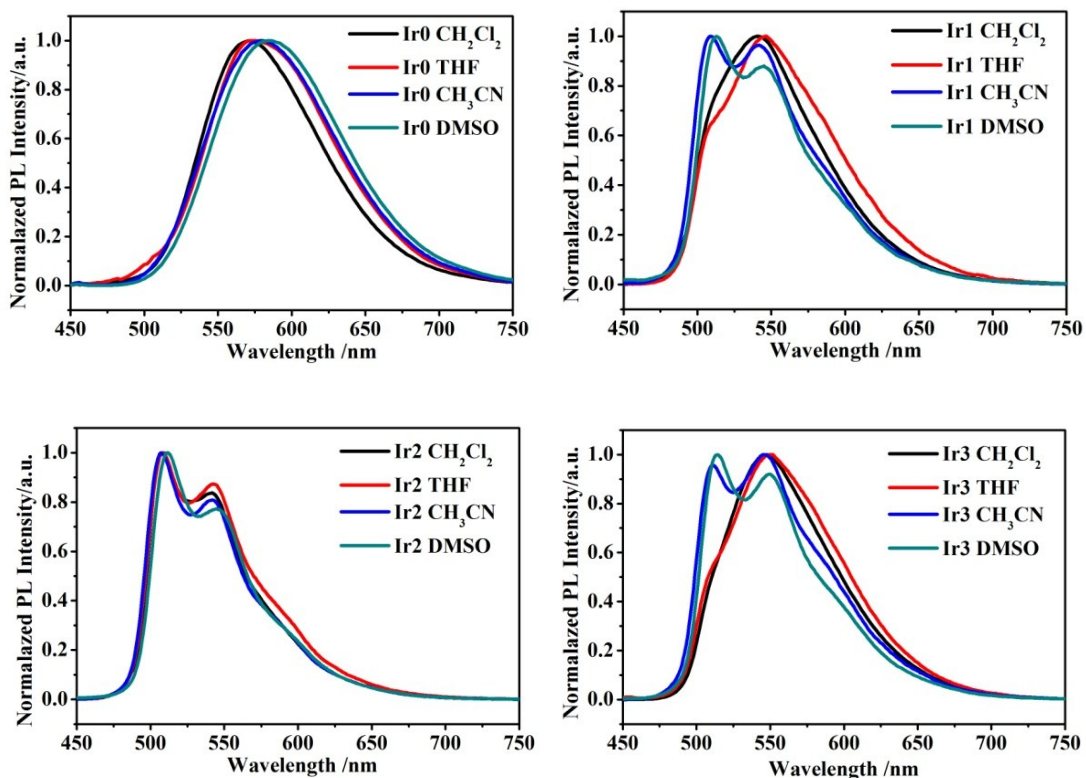
Fig. S4. Emission spectra of the **Ir0~Ir3** (λ_{ex} = 400 nm) in different solvents, at ambient temperature.
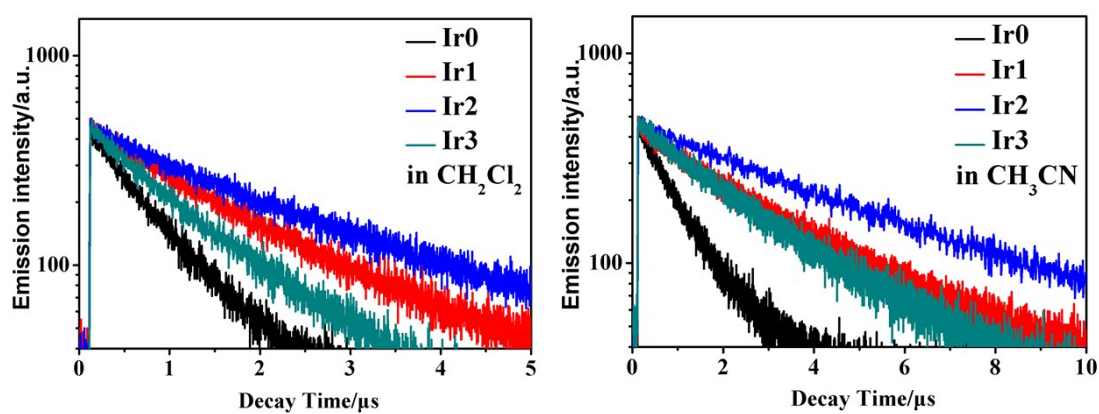

Fig. S5. Phosphorescence decay profiles of complexes **Ir0~Ir3** in degassed CH_2Cl_2 and degassed CH_3CN, at ambient temperature.

Table S2. Radiative rate constant and nonradiative rate constant of the Ir(III) complexes[a].

Ir complexes	$k_r(s^{-1}) \times 10^5$	$k_{nr}(s^{-1}) \times 10^5$
Ir0	2.87	9.63
Ir1	1.09	3.86
Ir2	1.23	2.01
Ir3	2.15	5.25

[a] Calculated from $k_r = \Phi_p \times \tau^{-1}$, $k_{nr} = \tau^{-1} - k_r$ in degassed CH_2Cl_2 solution.

Table S3. Parameters for the O_2-sensing film of the **Ir1** with different polymers as the supporting matrix (fitting of the result to the two-site model).

Ir1 complex (0.5 wt%)	f_1[a]	f_2[a]	K_{SV1}[b]	K_{SV2}[b]	r^2[c]	K_{SV}^{app}[d]	P_{O2}[e]
Ir1 (EC)	0.9625	0.0375	0.01003	0.0000	0.98891	0.00965	103.63
Ir1 (PCHC)	0.9515	0.0485	0.00090	0.0001	0.96966	0.00086	1162.79
Ir1 (PS)	0.9837	0.0163	0.00205	0.0000	0.97691	0.00202	495.05

[a] Ratio of the two portions of the iridium(III) complexes. [b] Quenching constant of the two portions. [c] Determination coefficients. [d] Weighted quenching constant, $K_{SV}^{app} = f_1 K_{SV1} + f_2 K_{SV2}$. [e] The oxygen partial pressure at which the initial emission intensity of the film is quenched by 50% and calculated as $1/K_{SV}^{app}$, in Torr.
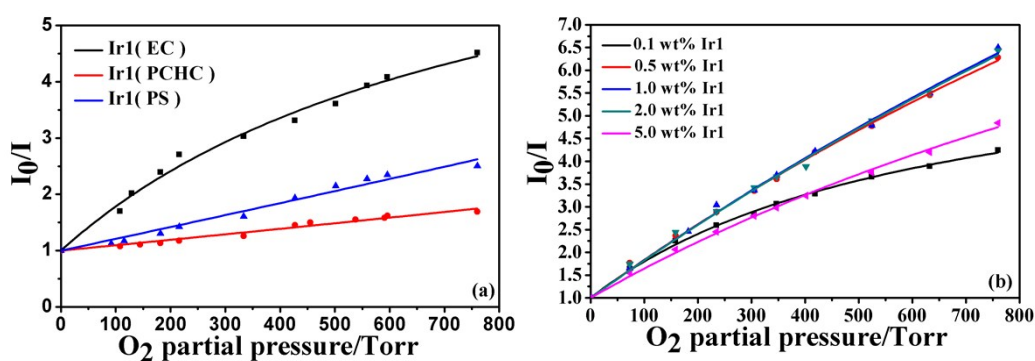

Fig. S6. (a) Stern-Volmer plots (intensity ratios I_0/I versus O_2 partial pressure) of **Ir1** (0.5 wt%) immobilized into different oxygen sensing films; (b) Stern-Volmer plots of the different content of **Ir1** in **EC** film, at ambient temperature.

Table S4. Parameters for the O_2-sensing film of the different content iridium(III) complexes with **EC** as the supporting matrix (fitting of the result to the two-site model).

Ir1 complex (wt%)	f_1[a]	f_2[a]	K_{SV1}[b]	K_{SV2}[b]	r^2[c]	K_{SV}^{app}[d]	P_{O2}[e]
0.1 wt% **Ir1**	0.85387	0.14613	0.01083	0.0001	0.99772	0.00625	160.00
0.5 wt% **Ir1**	0.96251	0.03749	0.00895	0.0000	0.99790	0.00861	116.14
1.0 wt% **Ir1**	0.97035	0.02965	0.00873	0.0001	0.99692	0.00847	118.06
2.0 wt% **Ir1**	0.96942	0.03058	0.00871	0.0001	0.99603	0.00844	118.48
5.0 wt% **Ir1**	0.93360	0.06640	0.00721	0.0001	0.99738	0.00674	148.37

[a] Ratio of the two portions of the iridium(III) complex **Ir1** [b] Quenching constant of the two portions. [c] Determination coefficients. [d] Weighted quenching constant, $K_{SV}^{app} = f_1 K_{SV1} + f_2 K_{SV2}$. [e] The oxygen partial pressure at which the initial emission intensity of the film is quenched by 50% and calculated as $1/K_{SV}^{app}$, in Torr.
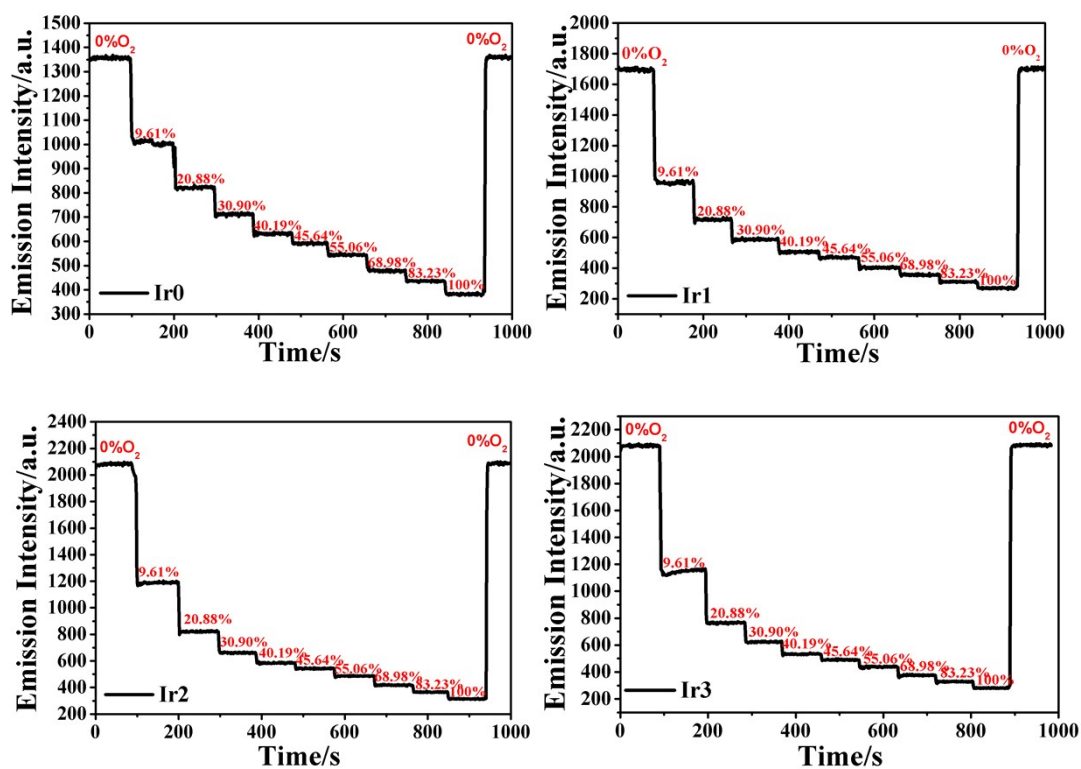
Fig. S7. Variation of the emission intensity of **Ir0~Ir3** incorporated into **EC** with the oxygen concentration.

Table S5. Lifetime Data for **Ir0~Ir3** [a].

Ir complexes	τ (ns)					
	0% O_2	2.17% O_2	3.38% O_2	5.11% O_2	7.06% O_2	9.61% O_2
Ir0	1130.12	317.79	235.91	179.42	140.85	106.39
Ir1	3812.01	1108.53	729.75	504.58	352.34	296.32
Ir2	4569.79	1466.12	1105.58	761.36	530.53	419.06
Ir3	3210.56	758.77	545.03	381.45	271.97	206.91

[a] The lifetime (τ) in CH_3CN solution (1.0×10^{-5} M) on the different concentration of oxygen (0-9.61%) was measured at ambient temperature.
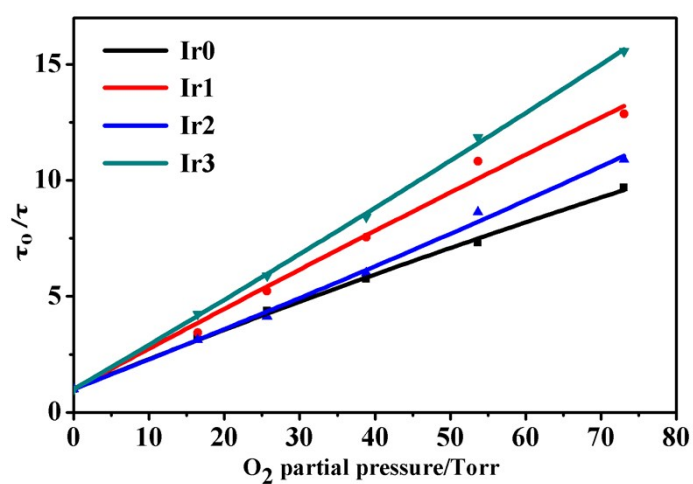
Fig. S8. Stern–Volmer plots (intensity ratios τ_0/τ versus O_2 partial pressure (0-9.61%)) of **Ir0~Ir3** in CH_3CN solutions (1.0×10^{-5} M)
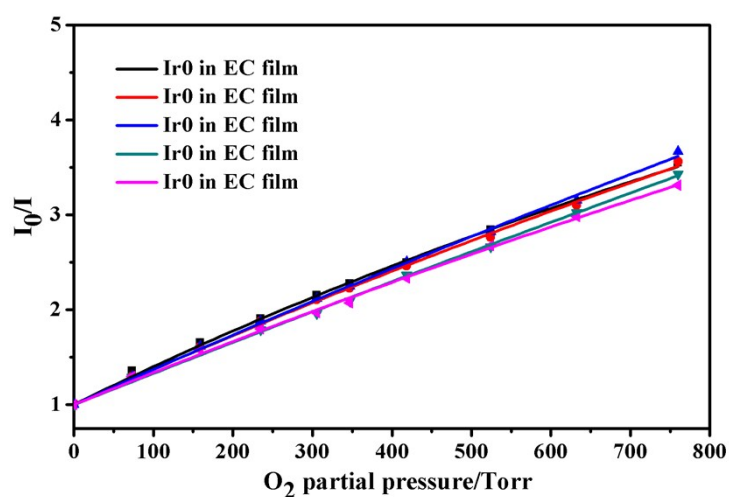
Fig. S9. The reproducibility tests of oxygen sensing films of **Ir0**.
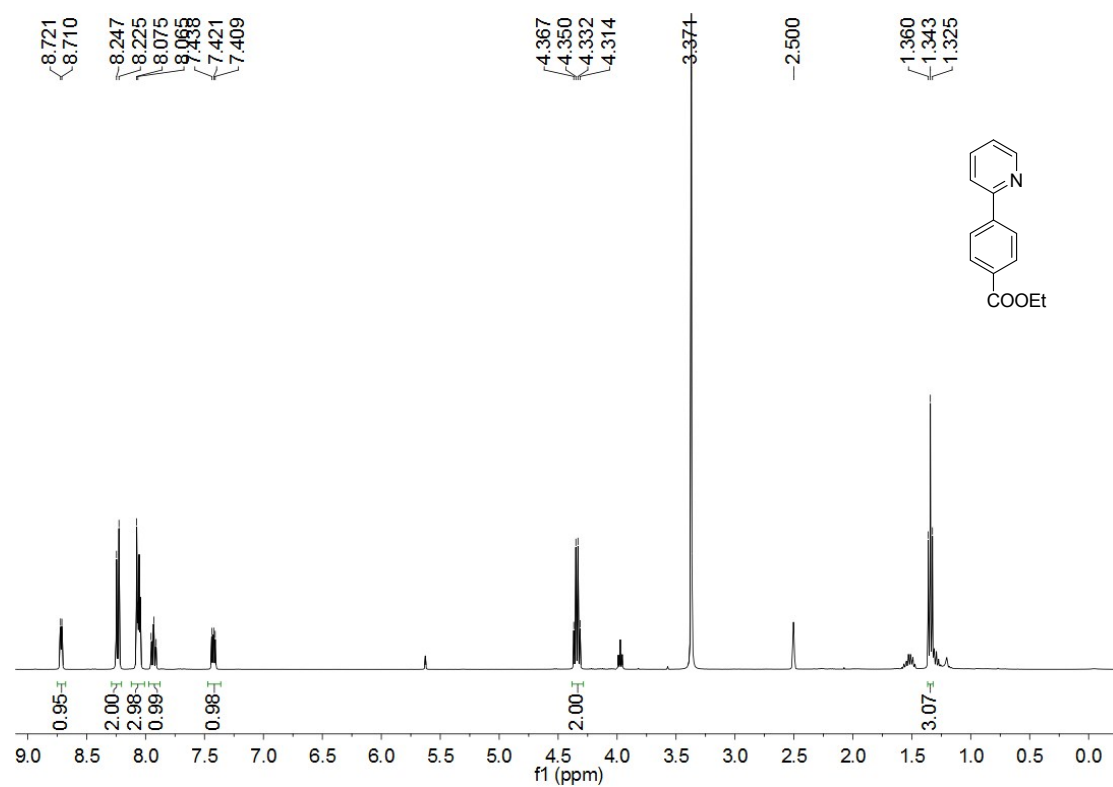
Fig. S10. The ^{1}H NMR spectrum of **epbz1** in DMSO-d_6.
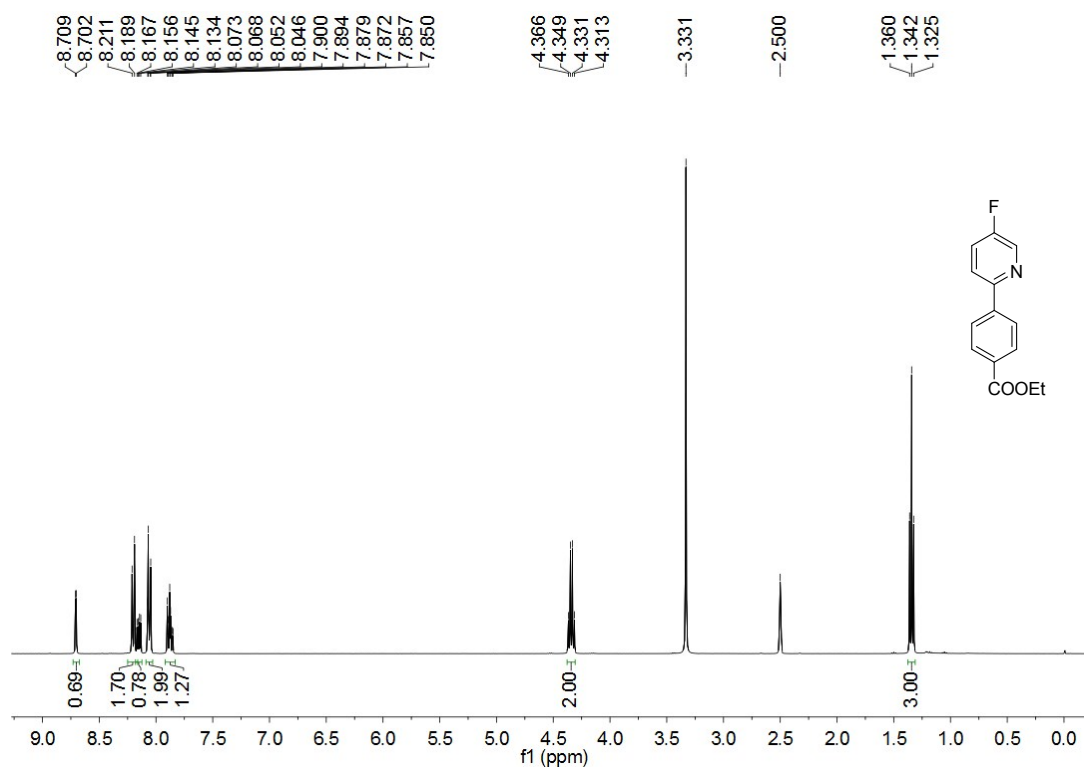
Fig. S11. The ^{1}H NMR spectrum of **epbz2** in DMSO-d_6.
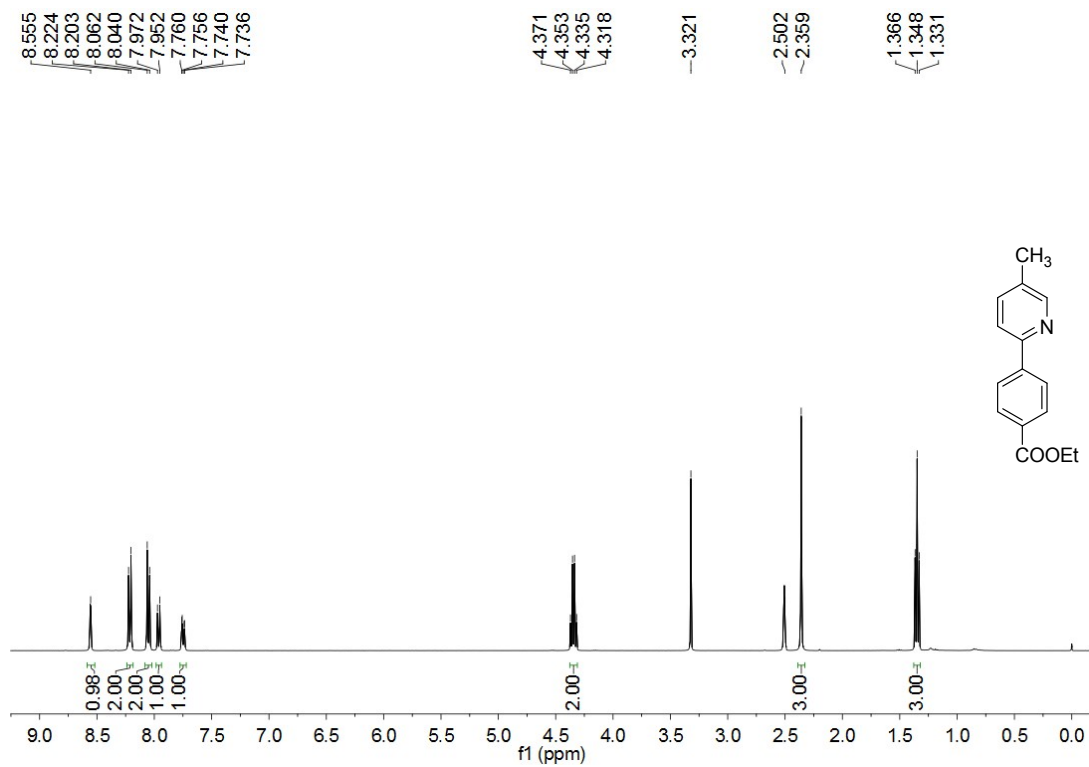
Fig. S12. The ^{1}H NMR spectrum of **epbz3** in DMSO-d_6.
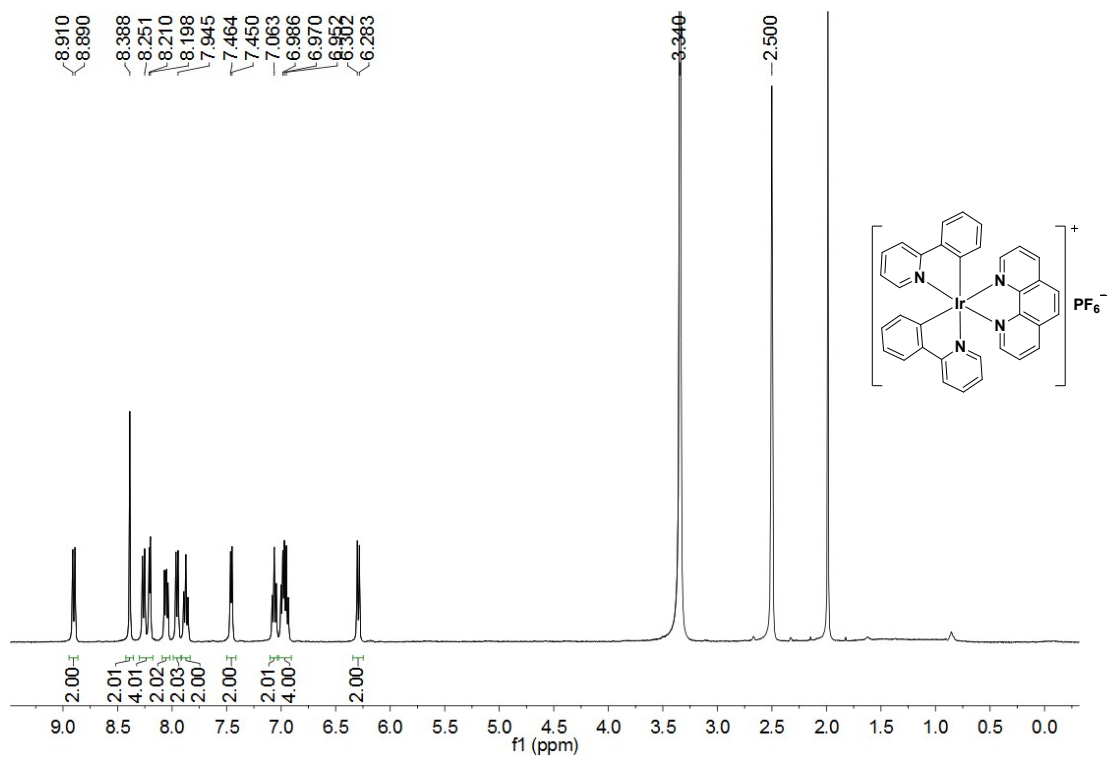
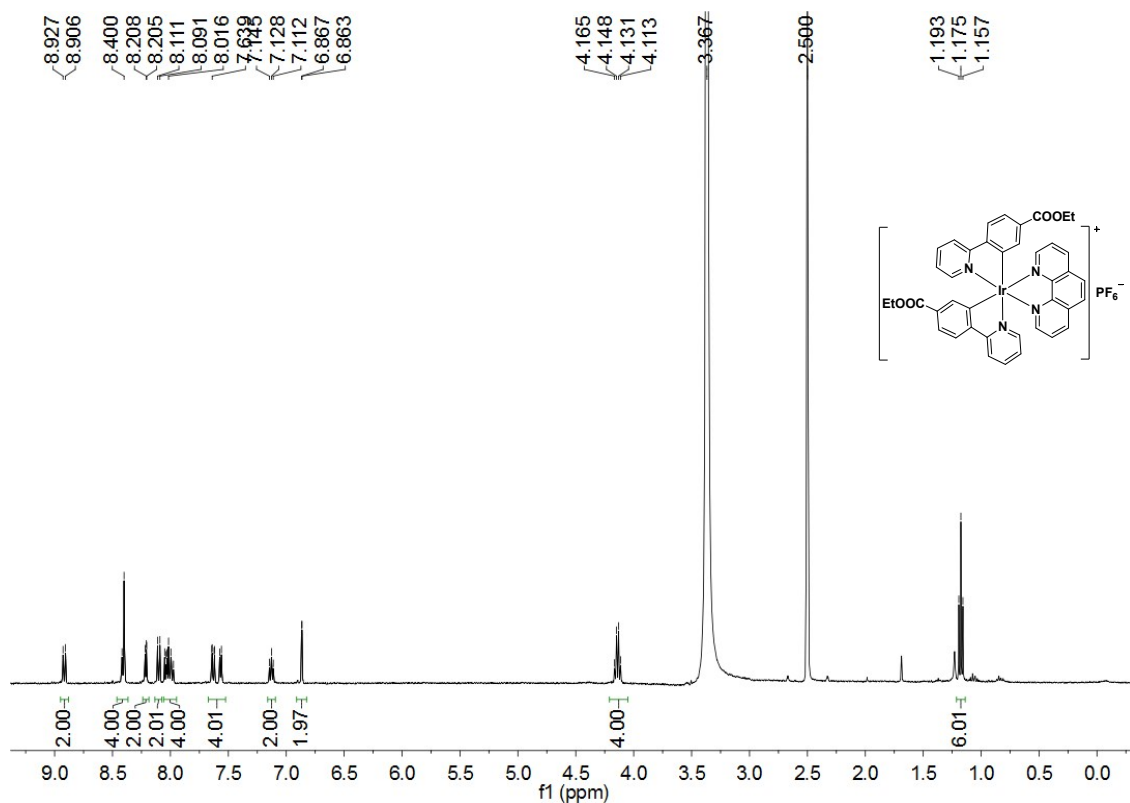**Fig. S13.** The ^{1}H NMR spectrum of **Ir0** in DMSO-d_6.

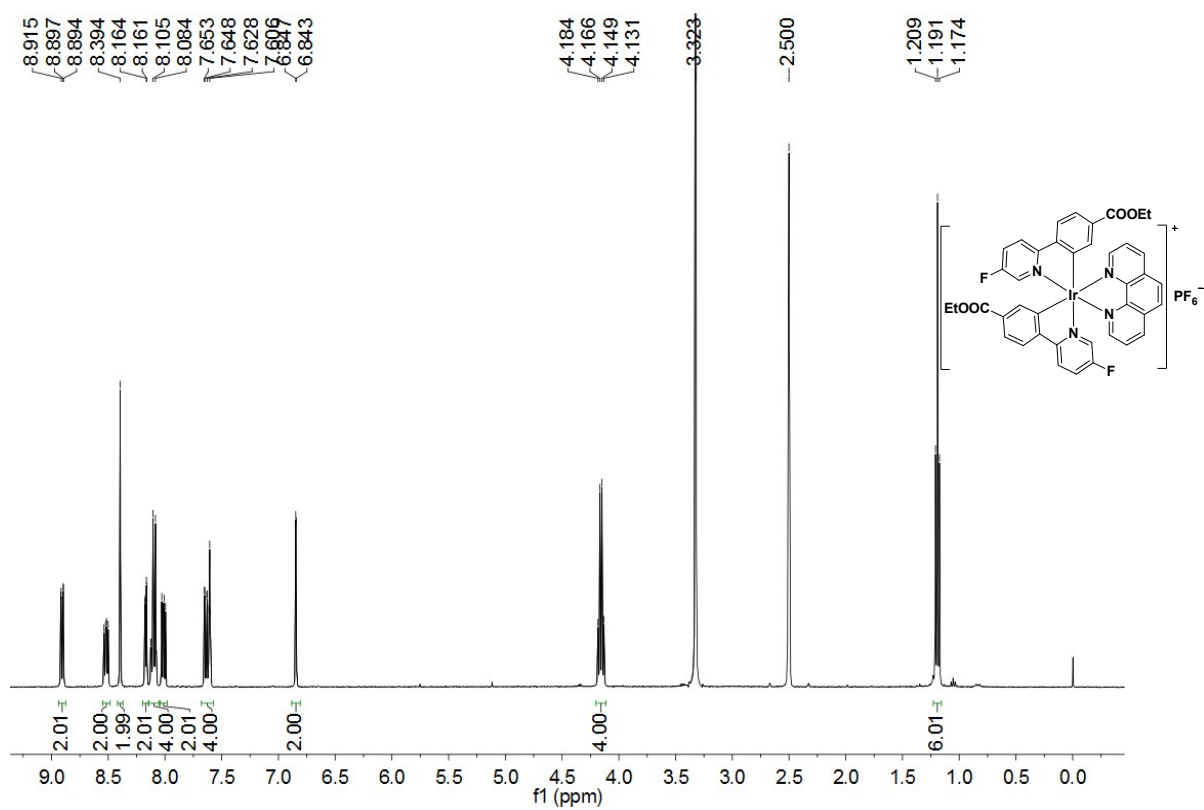**Fig. S14.** The ^{1}H NMR spectrum of **Ir1** in DMSO-d_6.

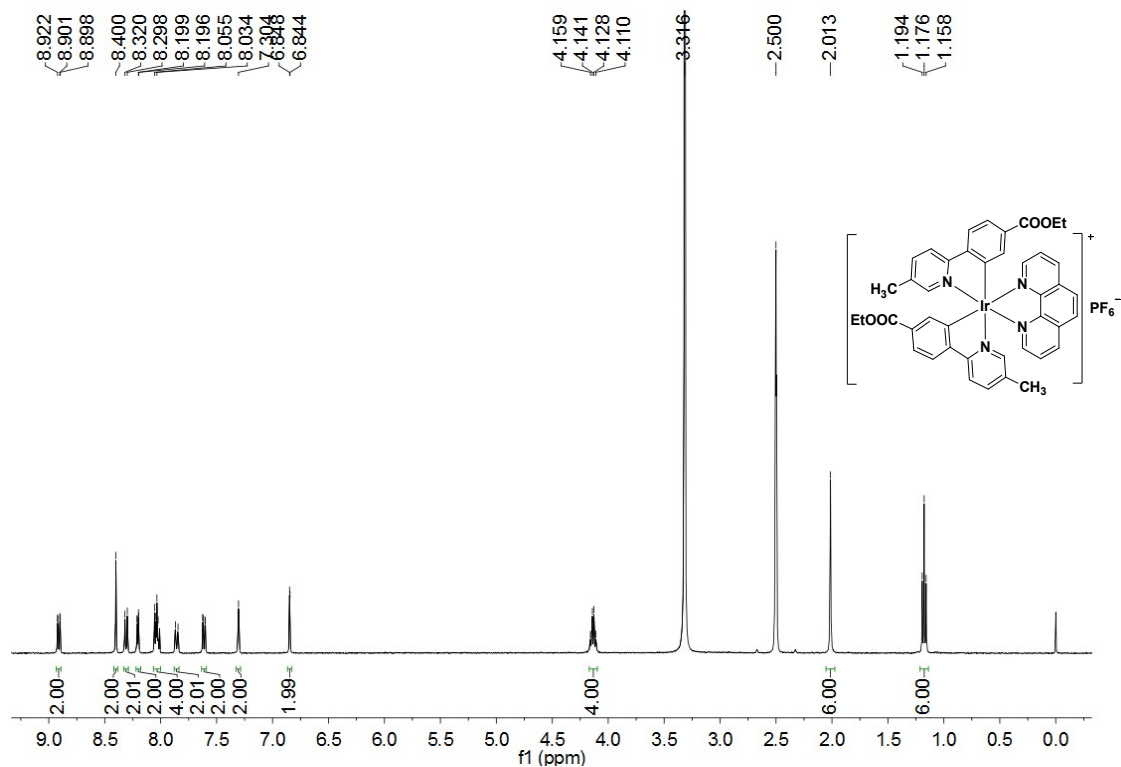**Fig. S15.** The ^{1}H NMR spectrum of **Ir2** in DMSO-d_6.

Fig. S16. The ^{1}H NMR spectrum of **Ir3** in DMSO-d_6.
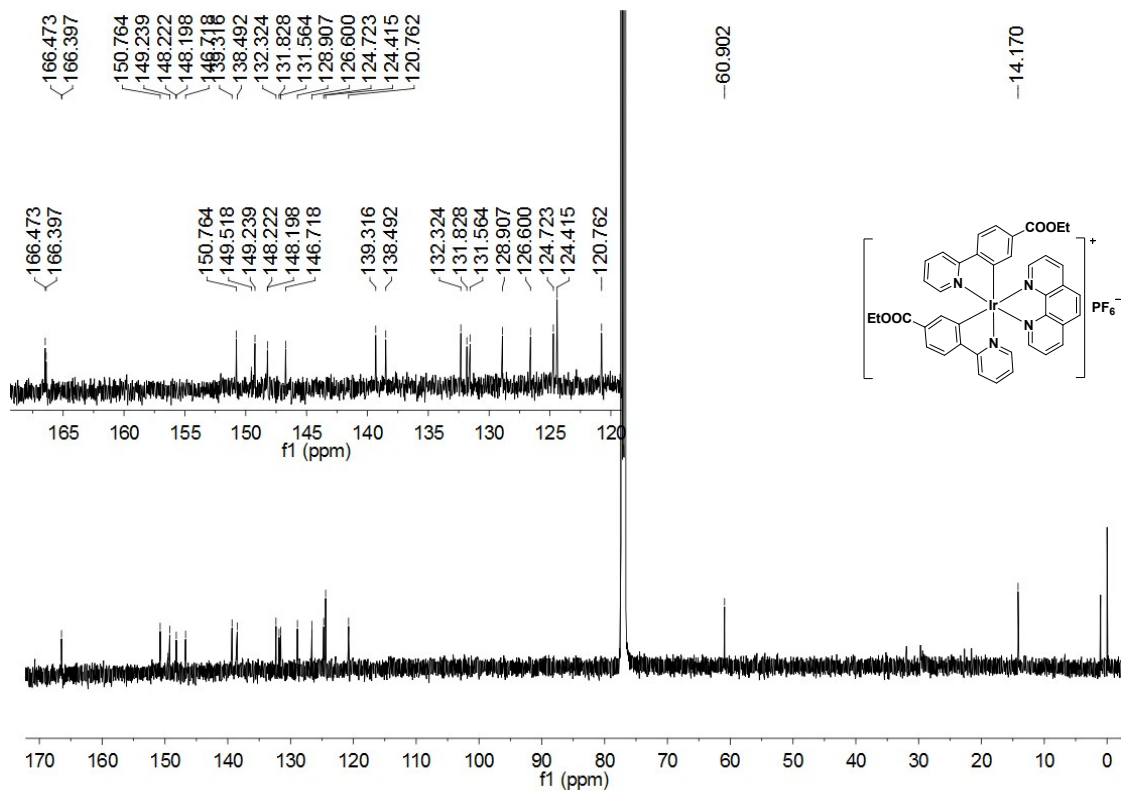
Fig. S17. The ^{13}C NMR spectrum of **Ir1** in DMSO-d_6.
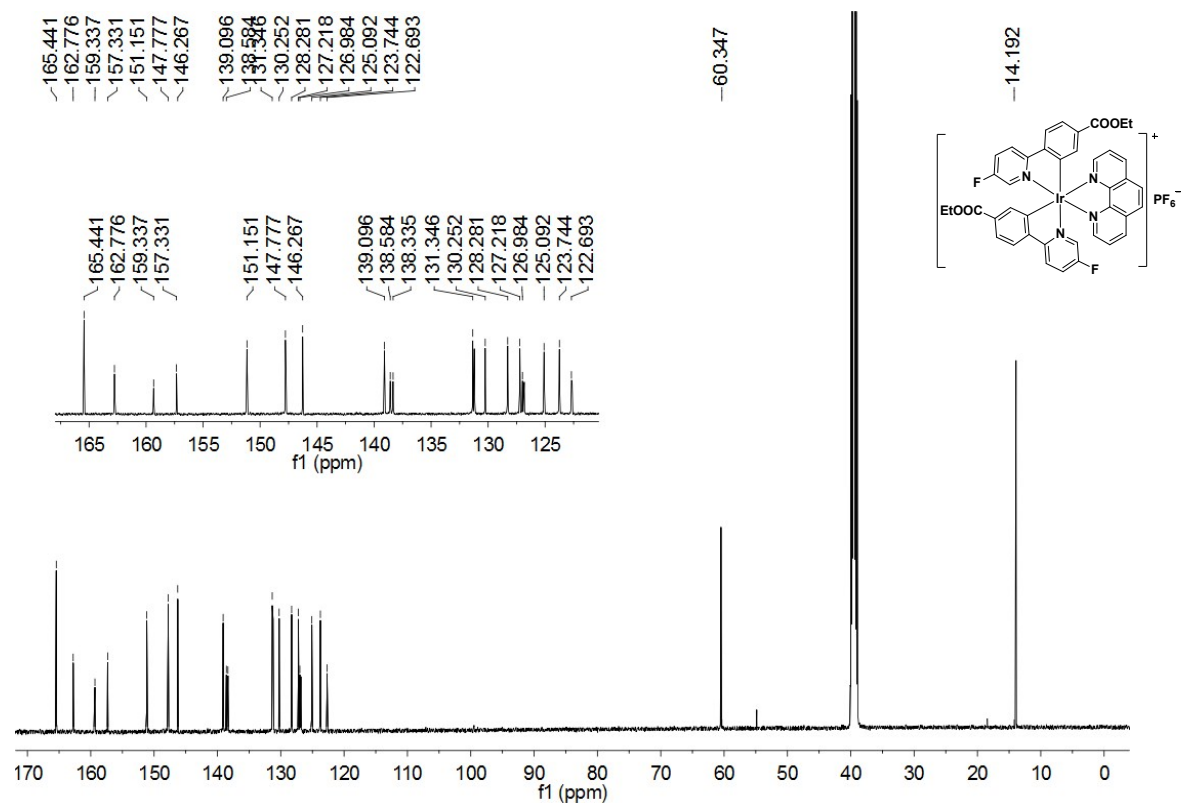
Fig. S18. The ^{13}C NMR spectrum of **Ir2** in DMSO-d_6.
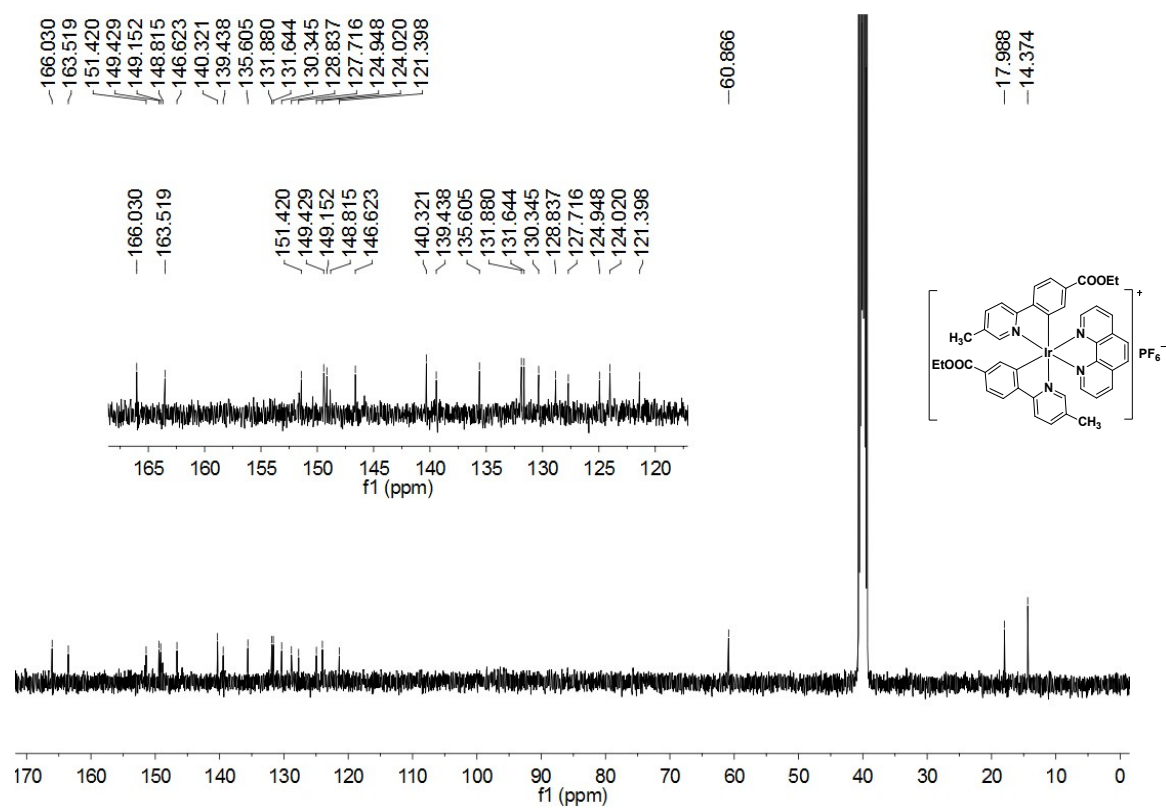
Fig. S19. The ^{13}C NMR spectrum of **Ir3** in DMSO-d_6.
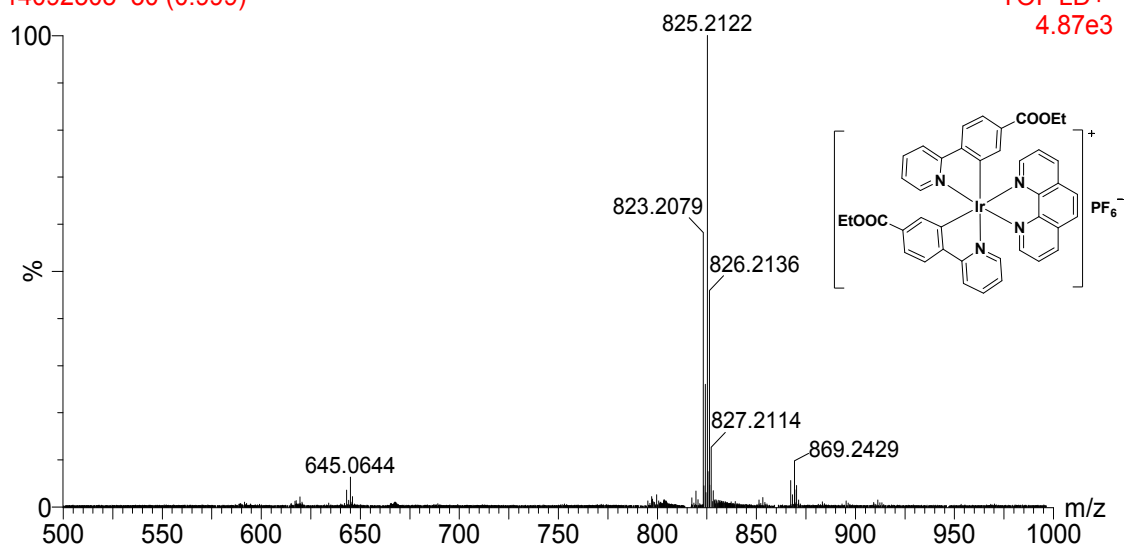
TOF LD+
4.87e3

Fig. S20. The HRMS (EI) of **Ir1**.
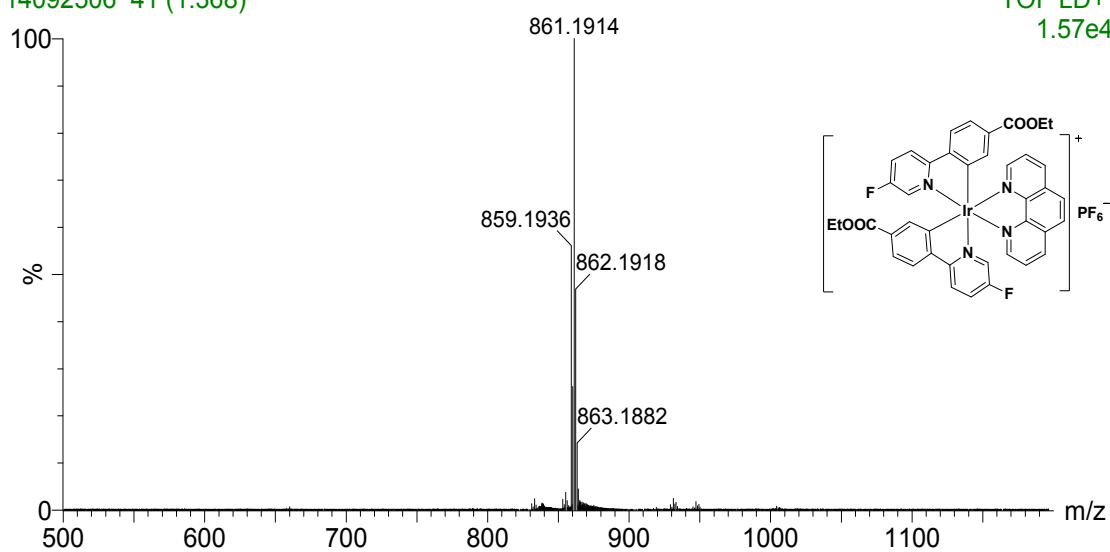
TOF LD+
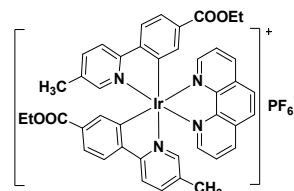1.57e4

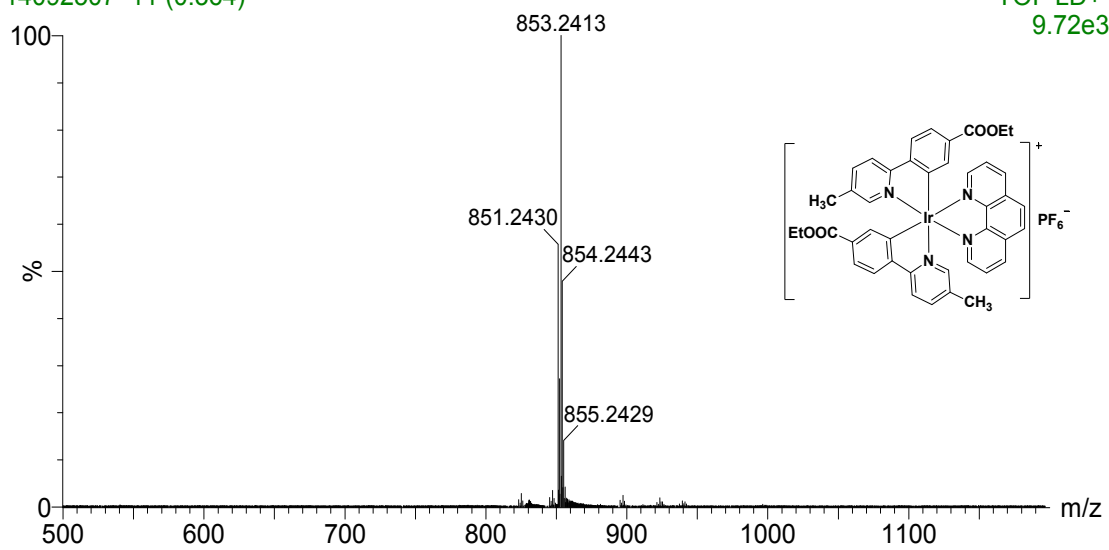**Fig. S21.** The HRMS (EI) of **Ir2**.

Fig. S22. The HRMS (EI) of **Ir3**.

References

[1] N. M. Shavaleev, F. Monti, R. D. Costa, R. Scopelliti, H. J. Bolink, E. Orti, G. Accorsi, N. Armaroli, E. Baranoff, M. Grätzel and M. K. Nazeeruddin, *Inorg. Chem.*, 2012, **51**, 2263-2271.